JAAS

Accepted Manuscript

This is an *Accepted Manuscript*, which has been through the Royal Society of Chemistry peer review process and has been accepted for publication.

Accepted Manuscripts are published online shortly after acceptance, before technical editing, formatting and proof reading. Using this free service, authors can make their results available to the community, in citable form, before we publish the edited article. We will replace this *Accepted Manuscript* with the edited and formatted *Advance Article* as soon as it is available.

You can find more information about *Accepted Manuscripts* in the Information for Authors.

Please note that technical editing may introduce minor changes to the text and/or graphics, which may alter content. The journal's standard Terms & Conditions and the Ethical guidelines still apply. In no event shall the Royal Society of Chemistry be held responsible for any errors or omissions in this *Accepted Manuscript* or any consequences arising from the use of any information it contains.

ROYAL SOCIETY OF CHEMISTRY

www.rsc.org/jaas

Impact of the chemical form of different fluorine sources on the formation of AlF molecules in a C_2H_2/N_2O flame

Jörg Acker[1)*], Stefan Bücker[1,2)] and Volker Hoffmann[2)]

[1)] Brandenburg Technical University Cottbus-Senftenberg, Faculty of Natural Sciences, Department of Chemistry, Großenhainer Straße 57, D-01968 Senftenberg, Germany

[2)] Leibniz Institute for Baltic Sea Research Warnemünde, Seestrasse 15, D-18119 Rostock, Germany

[3)] Leibniz Institute for Solid State and Materials Research Dresden (IFW Dresden), Helmholtzstraße 20, D-01069 Dresden, Germany

* corresponding author

Tel.: + 49-3573-85-839

Fax.: + 49-3573-85-809

e-mail: joerg.acker@b-tu.de

Abstract

The formation of diatomic AlF molecules was studied in the C_2H_2/N_2O flame by means of a high-resolution continuum source flame absorption spectrometer using the different fluorine containing compounds HF, H_2SiF_6, HBF_4 and CF_3COOH as fluorine sources. The fragmentation of these fluorine sources, as well the resulting impact on the AlF molecule formation, were derived from flame height distribution studies of the atomic and molecular species Al, AlO, Si, SiO, SiF, B and BF as a function of the fluorine concentration, the molar Al : F ratio and the burner gas composition. As a consequence, the used fluorine sources HF, H_2SiF_6, HBF_4 and CF_3COOH have been divided into two major groups. The first group of fluorine sources, covering HF, H_2SiF_6 and HBF_4, decompose during the drying of the aerosol under the formation of AlF_3, which is the dominating species for the transport of aluminium into the flame. Its decomposition into AlF results in a high sensitivity of the AlF molecular absorption at low flame observation heights. The second group of fluorine sources is exemplarily given by CF_3COOH. In the upper parts of the flame the cleavage of the very stable C-F bond proceeds incompletely so that the sensitivity of the AlF molecular absorption is considerably lower than that for the other fluorine sources. In consequence, the AlF molecules are formed by the reaction between the fluorine atoms and the aluminium atoms, which are transported into the flame without the aid of fluorine, presumably via oxidic and/or carbidic species. The present investigations show that the sensitivity of the AlF molecular absorption and the pathway of AlF formation depend on the chemical form of the fluorine in the studied samples.

1 Introduction

The reaction conditions that have to be present for the analytical determination of metals by means of flame or graphite furnace atomic absorption spectrometry (AAS) lead almost inevitably to the formation of diatomic molecules. Already without aspiration of any sample solution stable diatomic molecules like CN, NH and NO can be detected in the burner flame [1, 2]. The aqueous analyte solution and its matrix are the major source for the generation of a wide variety of diatomic molecules. Molecules consisting of non-metals only, such as NO, SO, CS or PO can be spontaneously formed by the decomposition of nitric, sulphuric or phosphoric acid, which are typical constituents of a sample solution. Furthermore, metal ions lead to diatomic molecules by a reaction with a flame or matrix constituents to produce mainly oxide or halide molecules. Of special importance are the quite stable diatomic molecules with an excitation and emission wavelength in the range of 200–800 nm. These molecules have the considerable potential to disturb the analytical determination of other elements. Their absorption or emission bands can interfere with the atomic absorption lines of several metals or with the spectral neighbourhood of these analyte elements, which affects the background correction. In another way, the formation of molecules as a parallel reaction can have a significant impact on the concentration of analyte atoms in the flame or the graphite furnace

However, the study of the diatomic molecules in the flame or the graphite furnace by means of atomic absorption spectrometer devices has become its own field of research as seen by the numerous early and very recent reviews on this topic [2-9]. In particular, the molecular absorption (MA) of diatomic molecules using a high resolution continuous absorption spectrometer device opens the pathway to the determination of non-metals, which cannot be analysed by their atomic absorption because of their inefficient excitation and their absorption or emission in the vacuum ultraviolet region. For this purpose, diatomic molecules of non-metals, which is particularly valid for the halides F, Cl, Br or I, need to be mutually generated by the addition of certain reagents, such as salts of Al, Ga, In, Mg, Ca, Sr or Ba in order to form stable diatomic molecules with one halide atom in the flame or the graphite furnace.

The present work is devoted to the distinct phenomena that a certain chemical species of a non-metal element can have a significant impact on the formation of diatomic molecules of this non-metal element. According to Templeton et al. [10], this approach has to be classified as species fractionation, which is defined as 'process of classification of an analyte or a group of analytes from a certain sample according to physical (e.g., size, solubility) or chemical (e.g., bonding, reactivity) properties'.

The first striking example of how a chemical species of an element affects the molecule formation is given by Huang et al. [11-13] who studied the carbon monosulphide (CS) molecular absorption at 258.056 nm in a conventional air-acetylene flame using high-resolution continuum source absorption spectrometry. They found that the CS molecular absorption strongly depends on the specific sulphur form; standard solutions of sulphite and sulphate, with the addition of acid, exhibit the same CS

molecular absorption sensitivity. Already, small amounts of hydrochloric or nitric acid added to the sulphite standard yields to a strong increase of CS molecular absorption sensitivity – up to a factor of 2.7– while the sensitivity of the sulphate standard remains unchanged with the acid concentration.

In the second striking example, Haraguchi et al. [14, 15] observed that the presence of hydrochloric acid significantly reduced the atomic absorption of In atoms compared to the HCl-free solution in both the air-acetylene flame and the nitrous oxide-acetylene flame. Replacing the HCl with $HClO_4$ lead to a further suppression of the In atomic absorption at identical acid concentrations. In both cases, the massive formation of InCl molecules caused the impact of the In atomic absorption. Furthermore, flame height distribution profiles showed that the InCl molecular absorption at 267.2 nm was higher for the HCl solution than that for the $HClO_4$ solution at a lower flame height, and that this effect reverses at a higher flame height positions. The authors explain this behaviour by different formation mechanisms of InCl. In HCl solution, the InCl is formed directly by the dehydration and pyrolysis of indium-chloro-complexes ($InCl_x(H_2O)_{6-x}^{3-x}$). This results in a high formation rate of InCl, and the InCl molecular absorption reaches its maximum at a low flame position. The formation of chlorine atoms out of the very stable perchlorate ions requires the cleavage of the Cl-O bonds. This process is comparably slow and requires a longer residence time in the flame. As a consequence, the maximum of InCl molecular absorption is found at a higher flame position.

The reverse is found in aluminium solutions with and without the addition of hydrofluoric acid [16-18]. In the absence of hydrofluoric acid, aluminium atoms are formed in the C_2H_2/N_2O flame via the reduction of volatile oxidic and/or carbidic species by the flame gases [19]. The presence of HF leads to volatile AlF_3, which vastly decomposes into AlF molecules and, subsequently, into Al atoms. The cleavage of AlF_3 releases Al atoms much faster than by the reduction of the oxidic and/or carbidic species. The total quantities of aluminium transported into the flame is almost identical, so the major difference between both pathways is a higher rate of Al atom formation by the cleavage of AlF_3 compared to the reduction of the oxidic and/or carbidic species in the absence of hydrofluoric acid.

The present study reveals that the transport pathway of aluminium into the flame, the pathway and flame position of AlF formation, and the molecular absorption of AlF depend on the chemical bonding state of the fluorine compounds used. These processes were studied by means of a high-resolution continuum source atomic absorption spectrometer to record the atomic absorption of Al, B and Si; the molecular absorption of AlF, BF, SiF; and the molecular emission of AlO as a function of the fluorine concentration; plus the molar Al : F ratio; the flame observation height; and the burner gas composition.

2 Experimental

2.1 Instrumentation and operating conditions

All measurements were carried out using a model contrAA 300 high resolution continuum source flame atomic absorption spectrometer (Analytik Jena, Jena, Germany), whose instrumental details are summarized by Welz et al. [2]. The experimental setup is identical to that in [18]. MA data of AlF at the wavelength 227.66 nm, of SiO at the wavelength 229.90 nm and of BF at the wavelength 195.59 nm, as well as AA data of Al at the wavelength 256.798 nm, B at the wavelength 249.77 nm and Si at the wavelength 251.61 nm were obtained by means of a reference spectrum to correct unwanted flame structures by static (AlF, BF, SiO) or dynamic (Al, B, Si) background correction with reference measurement. To record the molecular emission (ME) spectra of AlO at the wavelength of 484.23 nm, the light source was shut off by a shutter. Emission intensities are given as $Mcts \cdot s^{-1}$ (Megacounts per second), the unit of emission at contrAA 300. A baseline correction of the emission signals was done by static background correction. Data processing, background correction and statistics of the absorption and emission signals were identical to the detailed description given in [19]. The following operation conditions were chosen: a C_2H_2/N_2O flame with a constant 424 $L \cdot h^{-1}$ N_2O flow, 5 cm burner slot length and 9 $mL \cdot min^{-1}$ aspiration flow. Burner height and C_2H_2 flow are given in the text or figure captions.

2.2 Chemicals

All solutions were made from chemicals of p.a. quality ($Al(NO_3)_3 \cdot 9\ H_2O$, HF (w = 40% ($m \cdot m^{-1}$), CF_3COOH (w = 100% ($m \cdot m^{-1}$) from Merck, HBF_4 (w = 50% ($m \cdot m^{-1}$) from Acros, H_2SiF_6 (w = 40% ($m \cdot m^{-1}$) from Fluorchemie Dohna GmbH (Dohna, Germany)) and of deionized water (18 MΩ·cm resistivity, Seral, Ransbach-Baumbach, Germany). Stock solutions of the reagent (c_{Al} = 17 $g \cdot L^{-1}$) were prepared by solving solid $Al(NO_3)_3 \cdot 9\ H_2O$ in deionized water. The concentrations of the used HF and H_2SiF_6 stock solution were determined by frequent titration with 0.5 $mol \cdot L^{-1}$ NaOH (Titrisol® Merck Millipore, Watford, UK) using an automatic potentiometric titration system DL 70 ES (Mettler-Toledo, Greifensee, Switzerland). The HBF_4 concentration and the aluminium concentration in the stock solutions were determined by ICP OES (IRIS Intrepid II XUV, Thermo Fisher Scientific) measured in bracketing-mode using acid-matched standards prepared from single element standards (Merck). The CF_3COOH was taken from a freshly opened bottle.

2.3 Preparation of standards and solutions

All solutions and standards were prepared the same way. A certain amount of the fluorine source stock solution was weighed in the volumetric flask and almost filled to the top with deionised water. A

defined volume of an aluminium stock solution was added, and finally, the flask was filled up to the defined volume. It is necessary that the fluorine source, particularly in the case of HF, is diluted to its maximum in the volumetric flask before the Al solution is added. This prevents the precipitation of AlF_3 at fluorine concentrations > 6 $g \cdot L^{-1}$ or at high aluminium concentrations. The reversal procedure of adding HF to an Al solution gives the same insoluble precipitation.

3 Results and Discussion

3.1 Background study

As a first step, the background signals in the spectral neighbourhood of the relevant absorption and emission signals (see section 2.1) were studied for different flame observation heights and under a variation of the C_2H_2 flow rate for aluminium-free and aluminium-containing (c_{Al} = 1.7 g L^{-1}) solutions, each containing either 4 g·L^{-1} F as HF, HBF_4, H_2SiF_6 or CF_3COOH. HF, HBF_4 and CF_3COOH showed no significant background (except for a higher noise at the C_2H_2 flow rate of 190 L·h^{-1}) and no spectral interference with the AlF molecular emission bands. The same was valid in the range of the Al atomic absorption and the AlO molecular emission, which are not shown here. Only H_2SiF_6 caused strong background signals due to the SiO molecular absorption [8], which coincided partially with the AlF molecular absorption band at 227.66 nm (Fig. 1) and overlapped entirely with the Al atomic absorption line at 256.798 nm (Fig. 2). Only the AlO molecular emission at 484.23 nm was unaffected (not shown). In spite of these spectral interferences, the mentioned AlF and Al signals can be used for analytical purposes because of the following facts: (i) The SiO molecular absorption is independent from the Al concentration (not shown). (ii) The SiO molecular absorption signal is quite insensitive and changes only weakly with the H_2SiF_6 concentration (Fig. 2 and section 3.5). In a certain H_2SiF_6 concentration range, the SiO signal can be considered as constant. (iii) At a given H_2SiF_6 concentration, the SiO signals decrease significantly with increasing C_2H_2 flow rates (Fig. 1). (iv) The Al atomic absorption and the AlF molecular absorption increase strongly with increasing C_2H_2 flow rates (see section 3.4). Therefore, the peak area of the SiO molecular absorption bands can be determined in a separate measurement of an H_2SiF_6 solution and used for the background correction of Al + H_2SiF_6 sample solutions afterwards. Keeping these facts in mind, the absorbance of the partially overlapped AlF molecular emission can be reasonably determined for a low H_2SiF_6 concentration, a high C_2H_2 flow rate and, most significantly, by the choice of the limits for peak integration. If integration is done over a width of 5 pixels, the contribution of SiO to the AlF absorbance amounts to 17% for a C_2H_2 flow of 190 L·h^{-1}, to 6% for a C_2H_2 flow of 220 L·h^{-1} and to 2% for a C_2H_2 flow of 260 L·h^{-1}.

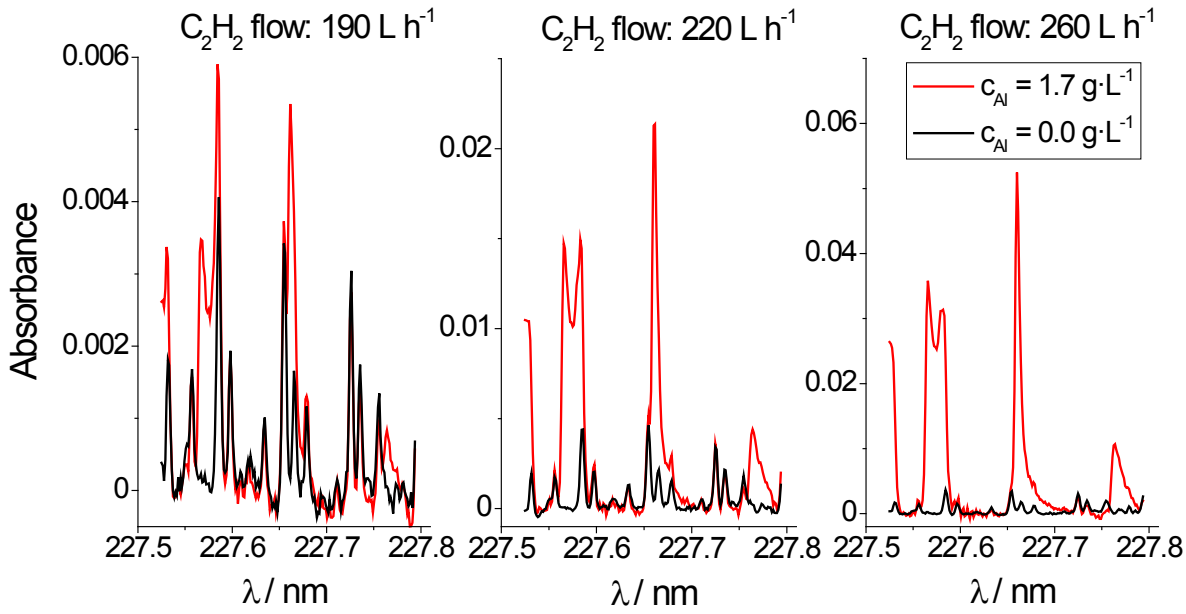

Figure 1: Absorption spectra in the wavelength range of the AlF molecular absorption around 227.66 nm measured for sample solutions with 4 $g \cdot L^{-1}$ F as H_2SiF_6 and either with aluminium (c_{Al} = 1.7 g L^{-1}) added (solid line) or without aluminium (empty markers). The spectra were recorded in a C_2H_2/N_2O flame at a flame observation height of 7 mm and at C_2H_2 flow rates of 190 $L \cdot h^{-1}$, 220 $L \cdot h^{-1}$ and 260 $L \cdot h^{-1}$.

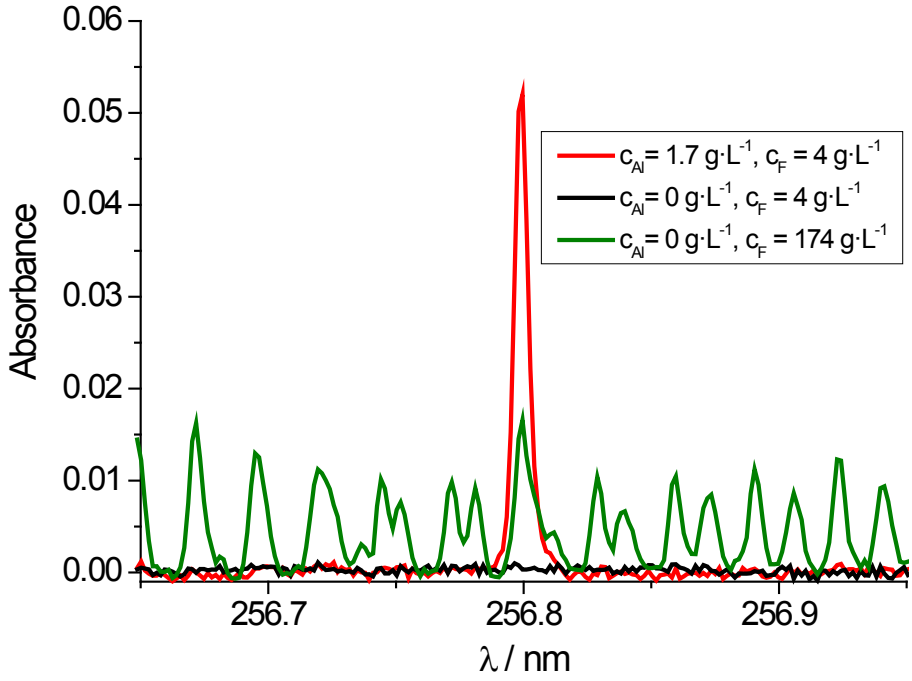

Figure 2: Absorption spectra of aluminium-free (empty markers) and aluminium-containing solutions (solid line), both containing fluorine as H_2SiF_6, recorded in a C_2H_2/N_2O flame at a flame observation height of 7 mm, and a C_2H_2 flow rate of 190 $L \cdot h^{-1}$ in the wavelength range of the aluminium atomic absorption at 256.798 nm.

3.2 Sensitivities of the AlF molecular absorption

Fig. 3 compares the AlF molecular absorption calibration curves using HF, H_2SiF_6, HBF_4 and CF_3COOH as fluorine sources, measured at a C_2H_2 flow of 260 $L \cdot h^{-1}$ and a burner height of 4 mm. The fluorine calibration curves of HF, HBF_4 and H_2SiF_6 consist of two linear sections of different slopes – the first one steeper compared to the second. The bend is associated with a change in the formation mechanism of AlF and is discussed in detail in [18]. In contrast, the fluorine calibration curve using a CF_3COOH source behaves linearly in the entire range between c_F = 0 $g \cdot L^{-1}$ and c_F = 16 $g \cdot L^{-1}$, and is significantly less steep than the calibration curves for the other fluorine sources.

The calibration curves show the significant dependence of the AlF molecular absorbance from the used fluorine source. The highest sensitivity is found for HF, closely followed by the curves for HBF_4 and H_2SiF_6 with only a slightly slower sensitivity. The weakest sensitivity is found for CF_3COOH as a fluorine source.

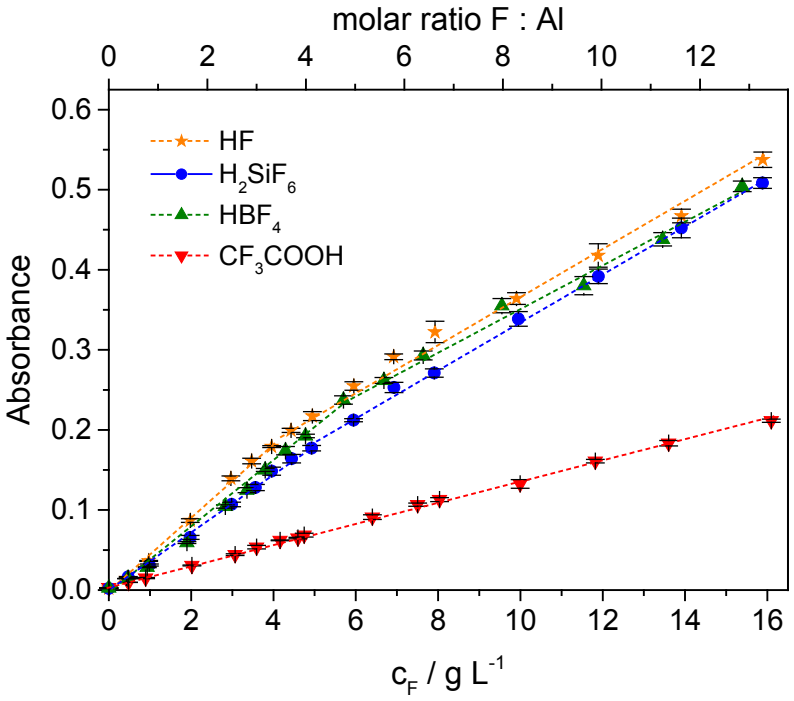

Figure 3: Calibration curves of the AlF molecular absorption at 227.66 nm of sample solutions containing aluminium (c_{Al} = 1.7 $g \cdot L^{-1}$) and different fluorine sources recorded at a C_2H_2 flow of 260 $L \cdot h^{-1}$ and a flame observation height of 4 mm.

3.3 Sensitivities of Al atomic absorption and AlO molecular emission

The atomic absorption of aluminium at 259.80 nm (Fig. 4a) as well as the molecular emission of AlO at 484.23 nm (Fig. 4b) were recorded at a flame observation height of 7 mm in a C_2H_2/N_2O flame (C_2H_2 flow of 220 $L \cdot h^{-1}$) using aluminium solutions of constant concentration (c_{Al} = 1.7 $g \cdot L^{-1}$) and increasing concentrations for each of the fluorine sources used.

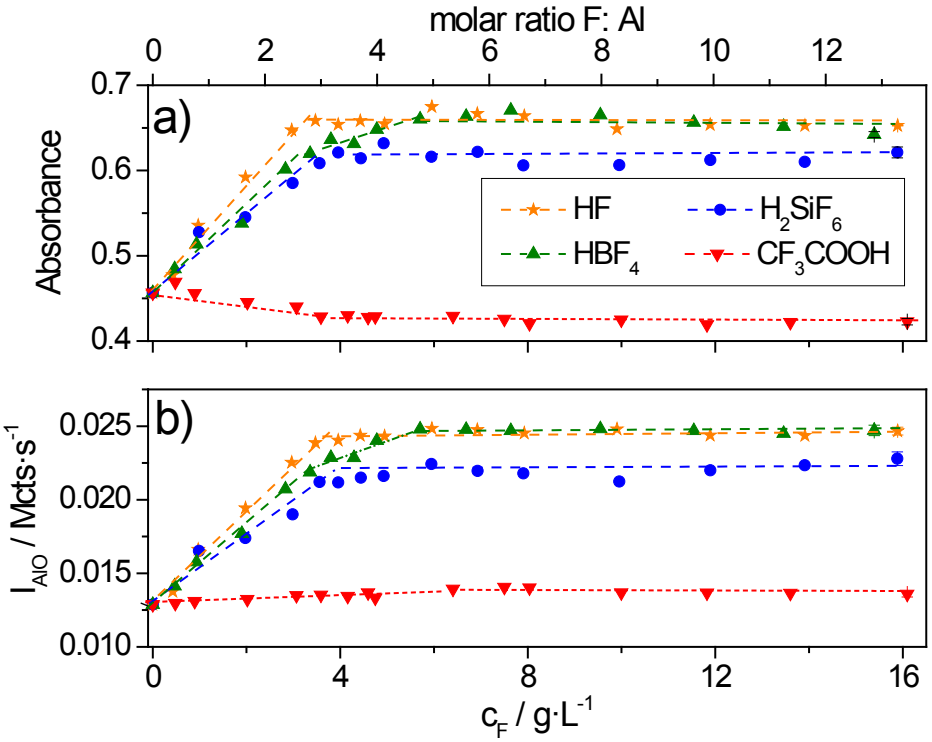

Figure 4: Al atomic absorption at 259.80 nm as function of the fluorine concentration (a) and AlO molecular emission intensity at 484.23 nm (b) as a function of the fluorine concentration generated by different fluorine sources, at c_{Al} = 1.7 $g \cdot L^{-1}$, a C_2H_2 flow of 220 $L \cdot h^{-1}$ and recorded at a flame observation height of 7 mm.

Fig. 4 shows the widely known effect of increasing Al intensity in the presence of hydrofluoric acid. In the case of HF as a fluorine source, the Al atomic absorption at 484.23 nm as well as the AlO molecular emission intensity at 484.23 nm increase linearly with the concentration of HF up to a molar ratio of F : Al around 3 and remains almost constant at the reached signal level at higher molar ratios. As recently shown [18], this behaviour is explained by the mechanism of Al and AlO formation. Below a molar F : Al ratio of 3 (*i.e.*, in excess of aluminium), two parallel pathways of aluminium atomization occur: (i) a fast pathway via the fractionation of volatile AlF_3 via AlF into Al; and (ii) a slow pathway suggested by Rubeska [19] via the reduction of the oxidic and/or carbidic species AlO_xC_y by the flame gas constituents. With the increasing molar ratio of F : Al, the quantity of aluminium transported into the flame as AlF_3 increases, whereas the quantity of aluminium transported as AlO_xC_y decreases. At a molar ratio above 3, Al is entirely transported by fluoride into the flame, presumably as volatile AlF_3

[18]. In conclusion, the presence of fluorine opens an alternative and faster pathway for Al atomization compared to the oxidic and/or carbidic pathway. It is merely a kinetic effect, because the total quantity of aluminium introduced into the flame is not changed by the presence of fluoride [18].

However, by curves similar in shape, H_2SiF_6 and HBF_4 show a similar effect on Al-containing solutions with significantly reduced Al AA absorbance and AlO emission intensities in the slope region (Fig 4), and for H_2SiF_6 in the plateau region. The linear slope regions span for HBF_4 and H_2SiF_6 up to molar ratios of 4.7 and 3.3, respectively, until the region of constant Al absorption is reached. For the AlO emission, these parameters are almost identical. The deviation from the molar ratio F : Al of 3 for HBF_4 and H_2SiF_6 has to be explained by the decomposition pathways of these compounds discussed later in this work.

The most astonishing behaviour exhibits CF_3COOH, which is entirely different from that of HF, HBF_4 and H_2SiF_6. Fig. 4 indicates a slightly decreasing Al absorption (by a factor of 1.1) until the plateau is reached at a molar ratio F : Al around 3. In the case of AlO emission, the intensity slightly increases (by a factor of 1.04) and remains constant at a molar ratio of F : Al around 5.4. From Fig. 4, it is concluded that CF_3COOH has no significant impact either on the transport or on the atomization pathway of Al; aluminium solutions with CF_3COOH behave practically like a fluorine-free solution.

3.4 Height distribution profiles of the observed Al flame species

Fig. 5 shows the distribution profiles of Al, AlF and AlO recorded as the function of the flame observation height in a C_2H_2-N_2O flame for a fluorine-free aluminium solution (c_{Al} = 1.7 g·L^{-1}) as well as for identical concentrated aluminium solutions with a fluorine concentration of 2 g·L^{-1} each added as HF, H_2SiF_6, HBF_4 and CF_3COOH.

In the absence of fluoride, aluminium atoms are already present at the lowest flame observation height of 4 mm, followed by an increase in their concentration with the observation height up to the maximum. Passing the maximum, the absorption lessens significantly for C_2H_2 flow rates of 190 L·h^{-1} and 220 L·h^{-1}. An increasing C_2H_2 flow rate shifts the maximum absorbance from an observation height of 6 mm for 190 L·h^{-1} and 220 L·h^{-1} to 10 mm for a C_2H_2 flow rate of 260 L·h^{-1}. Such a high flow rate stabilizes a considerable amount of Al atoms even at 16 mm height due to the low oxygen partial pressure in the flame. In the absence of fluoride, the AlO molecule is already present at a height of 4 mm. The emission intensity increases with the observation height and reaches a stable level at around 10 mm. Again, as lower the oxygen partial pressure in the flame is as lower is the observed AlO emission intensity so that AlO is no longer detectable at a C_2H_2 flow rate of 260 L·h^{-1}.

The acids HF, H_2SiF_6 and HBF_4 generate height distributions of identical shapes for Al, AlF and AlO. These acids increase the Al atomic absorption and shift their maximum to a lower observation height compared to the fluorine-free solution. With the increasing C_2H_2 flow rate, the maxima are shifted to higher observation heights and the Al atom concentration increases due to the lower oxygen partial

pressure. Although the Al and AlF height distributions exhibit the same shape, the AlF profile is always slightly shifted to lower observation heights by about 1 mm. The AlF molecules are already formed below the minimum observation height of 4 mm so that AlF is the precursor that decomposes under the formation of Al atoms. Finally, the highest species concentrations are always found for HF followed by H_2SiF_6 and finally by HBF_4, which underlines that, in the case of the latter two acids, other fluorine-containing species have to be present in the flame.

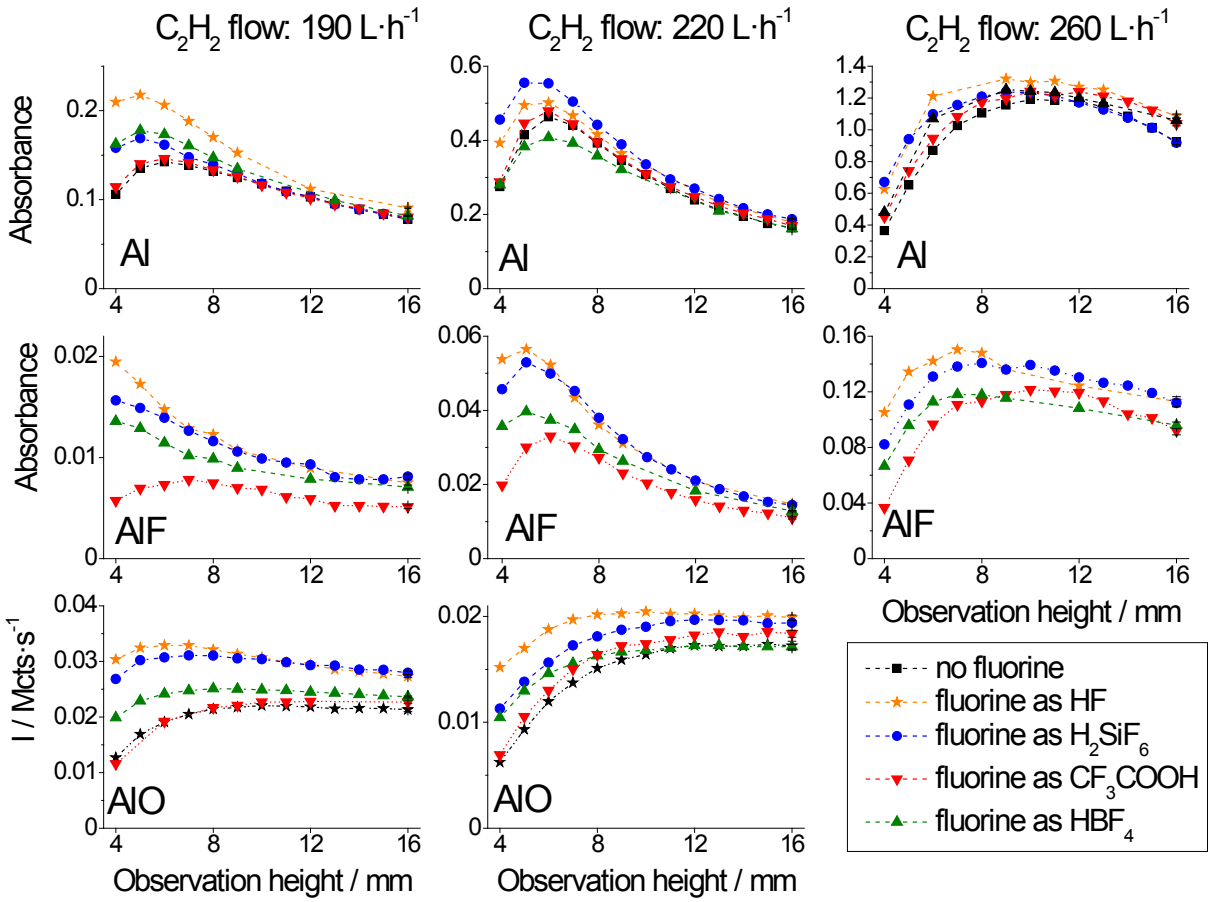

Figure 5: Al atomic absorption at the wavelength 256.798 nm, AlF molecular absorption at the wavelength 227.66 nm and AlO molecular emission at the wavelength 484.23 nm measured for c_F = 2 g·L^{-1} and c_{Al} = 1.7 g·L^{-1} (molar ratio F : Al = 1.7) and plotted as a function of the flame observation height.

CF_3COOH behaves as an exception, compared to the other studied acids, because it seems to release only a very low fraction of fluorine. This explains the almost identical curves for the Al atomic absorption for the fluorine-free solution and solutions with CF_3COOH. The only hint for the presence of fluorine in the flame can be derived from the very slight shift of the latter curve to higher absorbance's. The curves for the AlF molecular absorbance originated by the acids HF, H_2SiF_6 and HBF_4 are always higher in absorbance and identically shift to a lower observation height compared to the curve generated with CF_3COOH as the fluorine source. In fact, the curves of the Al atomic absorption

height distribution from the fluorine-free solution are almost identical in shape and maximum position to the AlF molecular absorption curves generated from CF_3COOH. It is concluded that AlF is formed by the reaction of Al and F atoms in the flame.

3.5 Spectrochemical behaviour of H_2SiF_6

As shown in Fig. 5, H_2SiF_6 increases the concentration of Al atoms and AlF molecules in the flame by its fragmentation. To follow the decomposition pathway of H_2SiF_6 in the presence of aluminium, the height distribution of Si atoms and SiO molecules was studied (see Fig. 6).

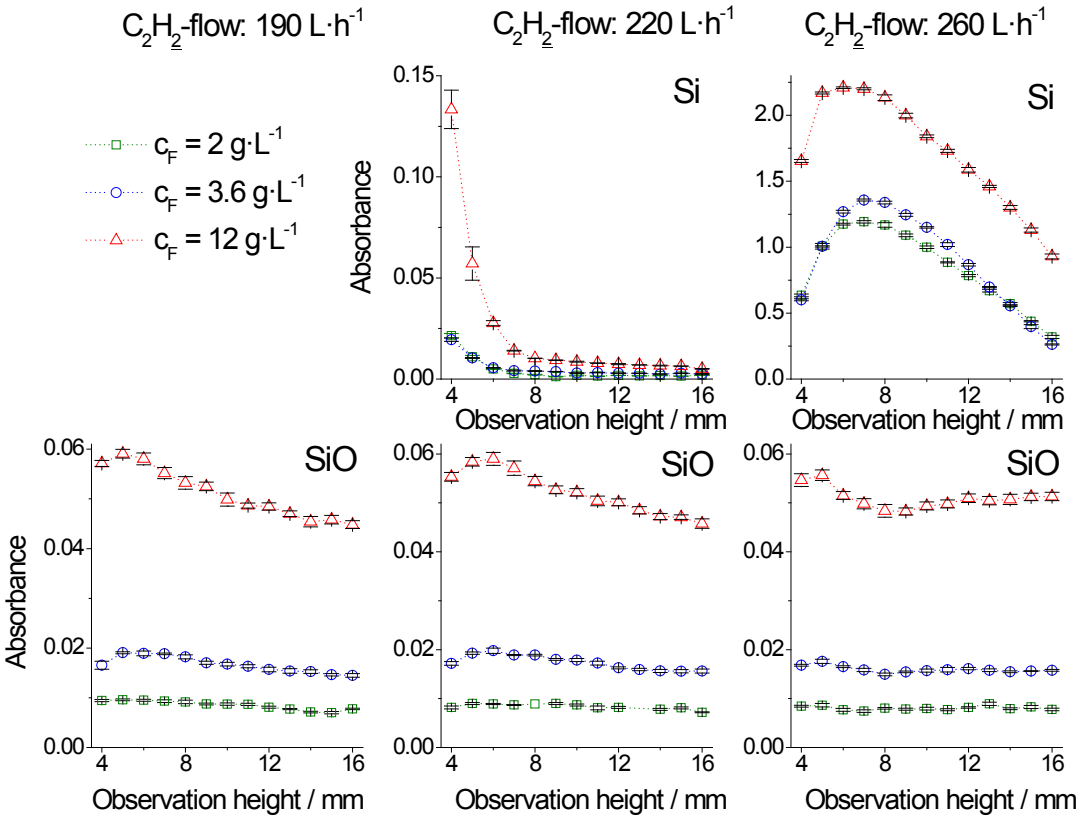

Figure 6: Si atomic absorption at the wavelength 251.61 nm, and SiO molecular absorption at the wavelength 229.90 nm recorded of aluminium-free and aluminium-containing (c_{Al} = 1.7 g·L^{-1}) solutions without H_2SiF_6 in different concentrations plotted as a function of the flame observation height.

At the lowest studied C_2H_2 flow rate of 190 L·h^{-1}, Si atoms were not detected. They were found to be present at 220 L·h^{-1} only at the very low flame observation heights of 4 mm and 5 mm. It requires a high C_2H_2 flow rate of 260 L·h^{-1} in order to measure a significant Si atomic absorption having its maximum at a height around 7 mm. In contrast, the SiO molecular absorption remains almost constant within the studied variations in the C_2H_2 flow rate and the flame observation height. An increase of the H_2SiF_6 concentration in the sample solution does not change the distribution profiles of the studied Si (Fig. 6) or Al (Fig. 5) species. However, any attempts failed to detect the SiF molecule in these solutions.

Therefore, the decomposition was studied with a H_2SiF_6 solution of higher concentrations in the absence of Al.

In agreement with Fig. 6, Fig. 7 shows that Si atoms require a minimum C_2H_2 flow rate of 220 $L \cdot h^{-1}$ and a low flame observation height of 4 mm to be observed. The degree of the total decomposition of H_2SiF_6 into Si atoms increases with the C_2H_2 flow rate and with the flame observation height; again in agreement with Fig. 6. And finally, due to the high concentration, SiF molecules were detected. From the curves in Fig. 7, it is concluded that SiF formed subsequently to the appearance of Si atoms; SiF is not a precursor for the generation of Si atoms.

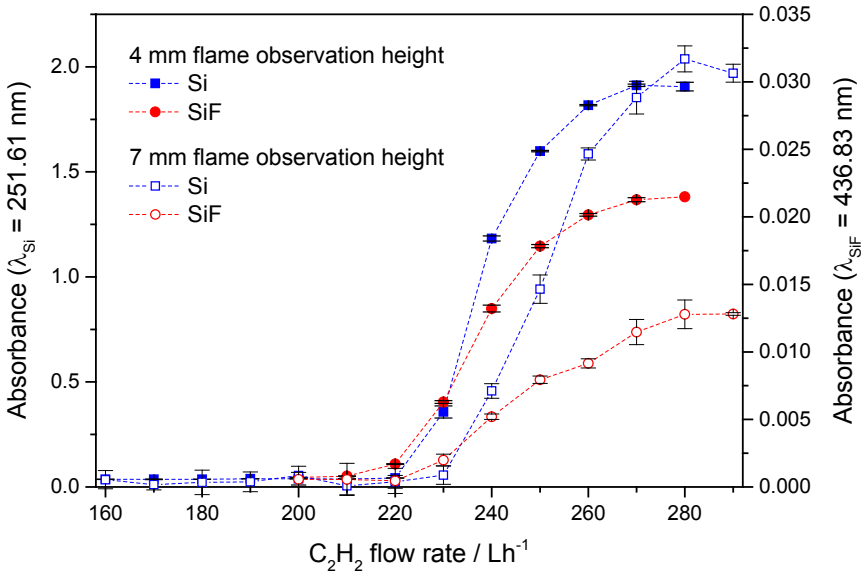

Figure 7: Si atomic absorption at the wavelength 251.61 nm and SiF molecular absorption at the wavelength 436.83 nm as a function of the C_2H_2 flow rate using a 16%(v/v) H_2SiF_6 measured at flame observation heights of 4 mm and 7 mm.

3.6 Spectrochemical behaviour of HBF_4

Fig. 5 has already shown that HBF_4 generates distribution functions for the Al and AlF flame species of identical shapes and maximum positions as those done by HF and H_2SiF_6. To study the HBF_4 fragmentation, the flame species B and BF were recorded at 249.773 nm and 195.589 nm, respectively, for solutions containing (i) HBF_4; (ii) HBF_4 and Al; and (iii) H_3BO_3 and CF_3COOH. Fig. 8a shows exemplarily for c_B = 1.71 $g \cdot L^{-1}$, c_F = 1.70 $g \cdot L^{-1}$, and a C_2H_2 flow rate of 260 $L \cdot h^{-1}$ that the presence of Al does not affect the formation of B atoms out of HBF_4. The same is valid for the BF molecules as seen by the identically shaped absorbance curves in Fig. 8b. Only the lower maximum absorbance of the HBF_4 + Al solution indicates that less F is bound as BF, although the total F concentration is identical to the HBF_4 solution without Al. It is difficult to derive the order of appearance of B and BF from Fig. 8 because of the only slight shift in the curve maxima. It might be interpreted that HBF_4 is firstly fragmented into BF followed by a very fast fragmentation under the liberation of B atoms.

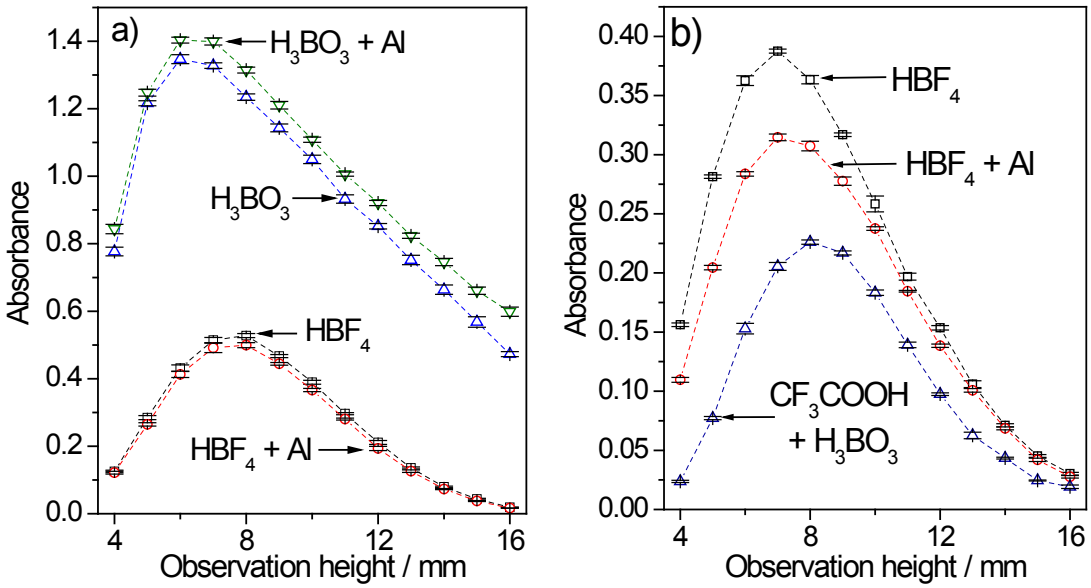

Figure 8: B atomic absorption at the wavelength 249.773 nm (a), BF molecular absorption at the wavelength 195.589 nm (b) recorded for solutions containing (i) HBF_4; (ii) HBF_4 and Al; and (iii) H_3BO_3 and CF_3COOH and plotted as a function of the flame observation height. (c_B = 1.71 g·L^{-1}, c_{Al} = 1.70 g·L^{-1}, C_2H_2 flow rate of 260 L·h^{-1}.)

It is useful to compare these results with the formation of B out of an H_3BO_3 solution of the same boron concentration and with or without Al added to it. As shown in Fig. 8a, H_3BO_3 generates a B atomic absorbance that is twice as high as that for HBF_4. Furthermore, the maximum B atomic absorbance is found at a height between 6 mm and 7 mm; about 2 mm lower than that for HBF_4. This is consistent with the known high volatility of boron oxides from boiling an aqueous solution of boric acid [20-22]. Keeping this in mind, the BF height profile generated by a solution containing H_3BO_3 and CF_3COOH (Fig. 8b) gives insight to its formation pathway: with the maximum of the BF molecular absorption around 8 mm flame observation height (the same value for AlF from CF_3COOH in Fig. 5) it is assumed that the decomposition of CF_3COOH requires a certain residence time in the flame. These fluorine atoms are then released into a flame that already contains B atoms leading to the formation of BF by the reaction of B atoms. This example marks the most significant difference regarding the AlF formation between CF_3COOH and the other studied fluorine sources, which originate from the bonding state of fluorine.

3.7 Classification of fluorine sources

The present study reveals that the AlF molecular absorbance depends on the bonding state of the used fluorine source. The sensitivity of the AlF molecular absorbance decreases for sample solutions with constant fluorine concentration at given aluminium concentration in the following order: HF > H_2SiF_6 > HBF_4 >> CF_3COOH. According to the presented height distributions of molecules and atoms in the flame, the studied fluorine sources can be divided into two major groups.

The first group, designated as the HF group, covers compounds in which gaseous HF is the major source for the formation of AlF. In the presence of HF, aluminium is transported into the flame as a volatile compound with a molar F : Al ratio of 3, presumably as gaseous AlF_3, according to the stoichiometric ratio derived from Fig. 4. Furthermore, this transport mechanism is characterized by the formation of AlF molecules already below the minimum flame observation height [18].

H_2SiF_6 and HBF_4 belong to this group because they show the same flame species distribution functions as obtained for HF-containing solutions. The key element is the formation of HF during the desolvatization of the sample aerosol according to Eq. 1 and Eq. 2 [23]. As a consequence, the formation of AlF out of H_2SiF_6 and HBF_4 occurs at the same low observation heights and with the same curve shapes as HF.

$$H_2SiF_6(aq) \xrightarrow{T} SiF_4(g) + 2HF(g) \quad (1)$$

$$HBF_4(aq) \xrightarrow{T} BF_3(g) + HF(g) \quad (2)$$

The always lower AlF molecular absorbance (Fig. 5) and the shifted bend position in Fig. 4 are explained by a lower amount of liberated HF out of H_2SiF_6 and HBF_4 solutions compared to solutions containing HF at the identical fluorine content. This behaviour is the consequence of the specific thermal behaviour of H_2SiF_6 and HBF_4. Parallel to the H_2SiF_6 decomposition into HF (g) and SiF_4 (g), the evaporation of water from the aerosol particles leads to the intermediary crystallization of solid salts of H_2SiF_6, presumably $Al_2(SiF_6)_3$. For the sake of simplicity, it is assumed that the thermal behaviour of those solid salts is identical to that of solid K_2SiF_6, a very well-studied model compound [24, 25]. K_2SiF_6 decomposes thermally always under the liberation of SiF_4 (g); however, the reaction behaviour is quite complex and depends on the partial pressure of H_2O (g) and HF (g) during the reaction. In the case of high H_2O partial pressures, decomposition into SiO_2 (s) and the formation of SiF_4 (g), SiF_3OH (g) and $F_3SiOSiF_3$ (g) are observed [24, 25].

It is assumed that the condition of high H_2O partial pressures occurs in the sample introduction system. Therefore, a considerable amount of fluorine is bound as SiF_4 (g), SiF_3OH (g) and $F_3SiOSiF_3$ (g), which leads to the observed shift in the bend positions in Fig. 4. These species decompose under flame conditions at higher observation heights and yield to silicon atoms. The observation, that the AlF molecular absorption of HF, H_2SiF_6 and HBF_4 becomes closer at high observation heights, may account for this. According to Fig. 7, SiF seems not to be a direct decomposition product from the fluorosilanes; SiF is presumably formed by the reaction of Si with F atoms in the flame.

HBF_4 shows a slightly different behaviour. According to Fig. 8a, B atoms seem to be earlier and more efficiently generated in the desolvation process out of a H_3BO_3 solution compared to HBF_4. Presumably, this is caused by the high volatility of boron oxides already in boiling boric acid solutions and by the high volatility of solid boric acid itself. Derived from the observation of AlF at the same low

flame observation height as for HF, the HBF_4 solution decomposes to a certain degree into HF during the desolvation of the aerosol particles. However, there is no striking evidence that Eq. 3 is not a valid model to describe the occurring processes at this stage of reaction; with respect to Fig. 8b one might argue that that the transport of B into the flame via the fluorine species seems to be more dominating than the pathway via the oxidic boron species:

$$HBF_4 \underset{+HF,-H_2O}{\overset{+H_2O,-HF}{\rightleftarrows}} HBF_3(OH) \underset{+HF,-H_2O}{\overset{+H_2O,-HF}{\rightleftarrows}} HBF_2(OH)_2 \underset{+HF,-H_2O}{\overset{+H_2O,-HF}{\rightleftarrows}} HBF(OH)_3 \underset{+HF}{\overset{-HF}{\rightleftarrows}} B(OH)_3 \qquad (3)$$

The decomposition of solid fluoroborates [26, 27] leads to the formation of metal fluorides and BF_3. Again, this pathway seems to take place in the flame and the B atoms seem to be formed out of BF_3 via BF molecules as intermediates, according to Fig. 8b. Again, not all fluorine present in HBF_4 is available for the formation of AlF_3 as it is in the case of HF. An incomplete fragmentation of the tetrafluoroborate anion (a high volatility of the boron-fluoro compounds) and the existence of BF, explain the observed deviation from the expected molar F : Al ratio of 3 in Fig. 4.

The second group of fluorine sources is represented by CF_3COOH, which stands exemplarily for organic compounds with stable C-F bonds. Due to its stability, it decomposes to a low degree only under the liberation of fluorine atoms. This has no noticeable impact on the transport mechanism of Al into the flame and on Al atomization, because the liberation of fluorine and subsequent AlF formation reaches its maximum at observation heights higher than that for the HF group compounds. This marks the first major difference: the CF_3COOH-containing sample solution behaves like the fluorine-free solution with respect to the Al atoms; that is, the transport of aluminium seems to be dominated by oxidic and/or carbidic aluminium species. The second major difference is found in the pathway that leads to AlF molecules: AlF is formed by the reaction of Al and F in the flame gas atmosphere. These circumstances of chemical stability of the C-F bond and the gas phase formation of AlF are the origin of the lower sensitivity of AlF molecular absorption and the slightly different height distribution function.

4 Conclusion

The present study shows how sensitively (i) the formation pathway of the diatomic AlF molecule and (ii) the magnitude of the molecular absorption are affected by the bonding state of several fluorine compounds. Ionic fluorine sources, as represented by aqueous solutions of HF, H_2SiF_6 and HBF_4, are characterized by a fast and complete decomposition that liberates the bound fluorine atoms, which immediately react under the formation of AlF molecules. However, depending on the structure of the ionic fluorine source, other fluorine-containing species, such as BF or SiF, are formed that slightly reduce the available amount of fluorine and, therefore, the flame concentration of AlF. The reaction pathway consisting of the transport of gaseous AlF_3 into the flame and its subsequent fragmentation to

AlF remains unaffected. In contrast, the cleavage of the very stable C-F bond requires a considerably longer residence of the organic fluorine compound in the flame; nevertheless, it proceeds only to a small extent. Therefore, the AlF molecular absorption is significantly weaker than for ionic fluorine sources, and the maximum AlF flame concentrations are found at higher flame observation heights. Organic fluorine sources have no impact on the transport pathway of aluminium, because fluorine atoms are generated by the C-F bond cleavage only at higher flame positions. Therefore, aluminium is presumably transported via the oxidic/carbidic species, and the observed AlF molecules are yielded by a reaction between Al and F atoms.

The presented results point to serious difficulties which can arise if the fluorine content should be analysed for samples with unknown total fluorine content and with unknown fluorine species. Such quantification would require calibration standards which have to be matched by the type of species and their respective fluorine content of that of the unknown sample composition. Such a demand appears practically not possible for unknown samples and consequently inaccurate results have to be expected. However, for very certain samples with known fluorine species and/or with knowledge about the total fluorine content strategies to distinguish between the different types of fluorine sources might be worked out based on their different molecular absorbance at a given fluorine concentration (Fig. 3 and Fig. 5) and at varying Al : F molecular ratios (Fig. 4).

5 Acknowledgement

This project is funded by the Ministry of Higher Education, Science and Culture of the State of Brandenburg and by the European Social Fund. We gratefully thank Dr H. Becker-Ross, Dr U. Heitmann, Dr M. D. Huang, Dr S. Florek and Dr M. Okruss from the ISAS Berlin for their manifold support of the present study by discussions; measurements with the prototypes of the high-resolution continuum source AA spectrometer; for access to their unique atomic and molecular spectral database; and for measurements of several survey spectra. Special thanks go to Dr D. Marquardt (Thermo Fisher Scientific GmbH) for the inspiring discussions. The authors thank our co-workers: Ms A. Voss for her general assistance, support and discussion during this work; Ms A. Voidel and Mr R. Buckan for ICP OES measurements; and Ms R. Keller and Ms A. Rietig for determination of the acid and anion concentrations by titration and ion chromatography, respectively.

References

[1] Welz, B.; Sperling, M. *Atomabsorptionsspektrometrie*, 4th revised edition, Wiley-VCH, Weinheim, 1997.

[2] B. Welz, H. Becker-Ross, S. Florek, U. Heitmann, *High Resolution Continuum Source AAS*, Wiley-VCH, Weinheim, Germany, 2005.

[3] K. Dittrich, Analytical applications of spectra of diatomic molecules, *Prog. Anal. At. Spectrosc.* 1980, **3**, 209–275.

[4] K. Dittrich, B. Vorberg, J. Funk, V. Beyer, Determination of some nonmetals by using diatomic molecular absorbance in a hot graphite furnace, *Spectrochim. Acta Part B* 1984, **39**, 349-363.

[5] K. Dittrich, Analysis by emission, absorption, and fluorescence of small molecules in the visible and ultraviolet range in gaseous phase, *CRC Crit. Rev. Anal. Chem.* 1986, **16**, 223–279.

[6] B. Welz, F.G. Lepri, R.G.O. Araujo, S.L.C. Ferreira, M.-D. Huang, M. Okruss, H. Becker-Ross, Determination of phosphorus, sulfur and the halogens using high-temperature molecular absorption spectrometry in flames and furnaces-A review, *Anal. Chim. Acta* 2009, **647**, 137–148.

[7] B. Welz, S. Morés, E. Carasek, M.G.R. Vale, M. Okruss, H. Becker-Ross, High Resolution Continuum Source atomic and molecular absorption spectrometry – A review, *Appl. Spectrosc. Rev.* 2010, **45**, 327–354.

[8] D.J. Butcher, Molecular absorption spectrometry in flames and furnaces: A review, *Anal. Chim. Acta* 2013, **804**, 1– 15.

[9] M. Resano, M. R. Flórez, E. García-Ruiz, Progress in the determination of metalloids and non-metals by means of high-resolution continuum source atomic or molecular absorption spectrometry. A critical review, *Anal. Bioanal. Chem.* 2014, **406**, 2239–2259.

[10] D.M. Templeton, F. Ariese, R. Cornelis, G. Danielsson, H. Muntau, H.P. van Leeuwen, R. Lobinski, Guidelines for terms related to chemical speciation and fractionation of elements: definitions, structural aspects and methodical approaches. *Pure Appl. Chem.* 2000, **72**, 1453–1470.

[11] M.D. Huang, H. Becker-Ross, S. Florek, U. Heitmann, M. Okruss; Direct determination of total sulfur in wine using a continuum-source atomic-absorption spectrometer and an air–acetylene flame, *Anal. Bioanal. Chem.* 2005, **382**, 1877–1881.

[12] M.D. Huang, H. Becker-Ross, S. Florek, U. Heitmann, M. Okruss; Determination of sulfur by molecular absorption of carbon monosulfide using a high-resolution continuum source absorption spectrometer and an air-acetylene flame, *Spectrochim. Acta Part B* 2006, **61**, 181–188.

[13] M.D. Huang, H. Becker-Ross, S. Florek, U. Heitmann, M. Okruss, C.-D. Patz, Determination of sulfur forms in wine including free and total sulfur dioxide based on molecular absorption of carbon monosulfide in the air–acetylene flame, *Anal. Bioanal. Chem.* 2008, **390**, 361–367.

[14] H. Haraguchi, K. Fuwa, Molecular absorption spectrum of InCl the flame, *Chemistry Letters* 1972, 913-916.

[15] H. Haraguchi, M. Shiraishi, K. Fuwa, Recombination reaction between indium and chlorine in air-acetylene flame observed by molecular flame absorption spectroscopy, *Chemistry Letters* 1973, 251-254.

[16] K. Konopicky, W. Schmidt, Die Emissionserhöhung des Aluminium-Flammenspektrums durch Fluoridionen, *Fresenius Z. Anal. Chem.* 1960, **174**, 262-268.

[17] A. Hofer, Über die Verwendung von Ammoniumfluorid bei der Bestimmung von Aluminium mittels Atom- Absorptionsspektrometrie in der Luft/Acetylen-Flamme, *Fresenius Z. Anal. Chem.* 1971, **253**, 206-207.

[18] J. Acker, S. Bücker, V. Hoffmann; The Formation of AlF Molecules and Al Atoms in a C_2H_2/N_2O Flame Studied by Absorption and Emission Spectrometry of Molecules and Atoms, *Curr. Anal. Chem.* 2014, **10**, 418-425.

[19] I. Rubeska, Interferences due to the solute volatilization in the nitrous oxide-acetylene flame. A generalized scheme, *Chem. Anal. (Warsaw, Poland)* 1977, **22**, 403-411.

[20] S. Böhlke, H. Ohlmeyer, Ch. Schuster, Determination of boron loss from boiling borate solutions in accident conditions in BWR plants, Annual Meeting on Nuclear Technology 2007, May 22 - 24, 2007, Karlsruhe, Germany, p. 437-440.

[21] S. Böhlke, H. Ohlmeyer, Ch. Schuster, A. Hurtado, Volatility of borates in boiling water reactors; Annual Meeting on Nuclear Technology 2008, 27.–29.05.2008, Hamburg, Germany, p. 301-304.

[22] S. Böhlke, *Untersuchungen zur Borflüchtigkeit bei der Einspeisung von Bor in SWR-Brennelemente bei transienten Kernzuständen*, Ph.D. Thesis, Technical University Dresden, **2010**.

[23] A.F. Hollemann, E. Wiberg, *Lehrbuch der anorganischen Chemie*, 101st edition, Walter de Gruyter, Berlin, **1995**.

[24] D. Menz, W. Wilde, L. Kolditz, Dynamisch thermische Analyse der Zersetzung von K_2SiF_6, *J. Fluorine Chem.* 1984, **24**, 345-354.

[25] L. Kolditz, V. Nitzsche, Zum Einfluss der Gasphase auf die thermische Zersetzung von K_2SiF_6, *Z. anorg. allg. Chem.* 1985, **526**, 48-54.

[26] J. Zachara, W. Wisniewski, Electronegativity force of cations and thermal decomposition of complex fluorides. II. Thermal decomposition of fluoroborates, *J. Thermal Anal.* 1995, **44**, 929-935.

[27] D. Nikolova, M. Georgiev, Synthesis, thermal investigations and kinetic data of $Zn(BF_4)_2 \cdot 6H_2O$; *J. Thermal Anal. Calorimetry* 2009, **95**, 319-321.